Journal of Applied Electrochemistry (2005) 35:1015–1024
DOI 10.1007/s10800-005-7340-7

Peroxide formation in a zero-gap chlor-alkali cell with an oxygen-depolarized cathode

LUDWIG LIPP[1,2], SHIMSHON GOTTESFELD[1,3] and JERZY CHLISTUNOFF[1,*]
[1]*Los Alamos National Laboratory, Los Alamos, NM, 87545, USA*
[2]*FuelCell Energy, Inc., Danbury, CT, 06813, USA*
[3]*MTI Microfuel Cells, Albany, NY, 12205, USA*
*(*author for correspondence: fax: +1-505-665-4292, e-mail: jerzy@lanl.gov)*

Received 19 September 2004; accepted in revised form 3 May 2005

Key words: chlor-alkali, gas diffusion electrode, membrane technology, oxygen-depolarized cathode, peroxide, sodium hydroxide

Abstract

The effects of various factors on the undesired generation of hydrogen peroxide in a zero-gap oxygen-depolarized chlor-alkali cell employing carbon-supported platinum catalysts were studied. The rate of peroxide generation was found to decrease with platinum loading and increase with current density. The quantity of peroxide generated also increased with electrolysis time, and reached a steady state value after a few 100 h of cell operation at 10 kA m^{-2}. The steady-state peroxide to hydroxide molar ratio was found to increase with brine concentration. This phenomenon is believed to originate from a decrease of water activity at the reaction site that accompanies the brine concentration increase. No correlation between chloride crossover and the concentration of peroxide generated was detected. It is postulated that carbon particles are predominantly responsible for the partial oxygen reduction and that their contribution increases with electrolysis time as a result of processes that render the carbon surface more hydrophilic.

1. Introduction

The development of the membrane chlor-alkali technology and its further optimization resulted in a significant cut of the energy consumption in chlor-alkali production. State-of-the-art membrane reactors operate at voltages as low as 3.2 V at a typical current density of 4 kA m^{-2} (0.4 A cm^{-2}) [1]. In spite of the effort to reduce the energy use by the chlor-alkali industry, the brine electrolysis is still one of the most energy-intensive industrial operations. It is believed that the mature membrane technology reached the theoretical limit on energy consumption. As a consequence, further optimization of this technology is not expected to result in meaningful energy savings. However, by replacing the hydrogen-evolving cathode in a membrane cell with an oxygen-depolarized cathode, the cell voltage and energy consumption can be reduced by as much as 30% at 4 kA m^{-2}.

The electrochemical reduction of oxygen in an alkaline medium has been the subject of several research studies [2–19] and the successful application of cathodes containing silver [20–22] and platinum [21, 22] catalysts in oxygen-depolarized chlor-alkali cells has been reported.

While oxygen-depolarized chlor-alkali cells significantly lower energy consumption per unit weight of chlorine and caustic product, they also have some shortcomings. These shortcomings result predominantly from the corrosion of cathode components, which can lead to the catalyst loss, electrode flooding, etc. Another drawback of oxygen cathodes in chlor-alkali cells is the relatively high stability of peroxide, an intermediate product in oxygen reduction. The loss of electrical energy for peroxide formation is of no concern, because the equivalent quantity of NaOH is formed upon peroxide decomposition. The potentially adverse effects of peroxide on cathode durability [23] and caustic handling issues make peroxide a troublesome byproduct. It is believed that the most significant contribution to peroxide generation by an oxygen-depolarized cathode (utilizing a carbon-supported noble metal catalyst) results from oxygen reduction on the carbon particles [24].

This paper presents part of our research on the implementation of oxygen-depolarized cathodes in chlor-alkali cells. It focuses on selected performance characteristics of the cells with an emphasis on peroxide generation. As our effort to implement gas diffusion cathodes in chlor-alkali cells originated from fuel cell

research [25], the designs of our chlor-alkali cells and fuel cells are quite similar. For instance, while the majority of oxygen-depolarized chlor-alkali cells [20, 22, 26–28] can be described as finite-gap or three-compartment (where the cathode compartment is separated by the gas-diffusion cathode into distinct oxygen and caustic chambers) we used a fuel cell-like, zero-gap configuration. In this configuration there are no separate oxygen and caustic chambers and the oxygen cathode remains in intimate contact with the ion-exchange membrane. In this way, both the flooding of the cathode by the NaOH solution and the ohmic drop have been significantly reduced.

2. Experimental

The cells used in this study (Figure 1) employed commercially available, 50 cm^2 double-sided gas diffusion electrodes (ELAT®) with a carbon-supported platinum catalyst (E-TEK). The catalyst layer contained either 80% or 20% of carbon-supported (Vulcan XC-72) platinum with a total Pt loading of 0.05 and 0.005 kg m^{-2} (5.0 and 0.5 mg cm^{-2}), respectively. The electrodes were separated from the membrane by a thin hydrophilic spacer (Panex® 30 carbon cloth, Zoltek). The gas diffusion layer of the cathode remained in contact with our proprietary gold-plated nickel or stainless steel (SS316) flow-field and gold-plated nickel or stainless steel (SS316) current collector. The anode consisted of two DSA® coated titanium meshes (mesh 120 and 60). An integrated single serpentine channel anode flow-field and current collector were made of DSA® coated titanium. The cell gaskets were made from ~1 mm or ~1.6 mm Goretex® Teflon tape. In order to maintain reproducible conditions at the membrane/electrode/flow-field interfaces, the cell bolts were torqued to a preset torque that resulted in an average membrane compression of 689 kPa (100 psi), as determined in a separate experiment with Pressurex® pressure sensitive film (Fuji Film).

The cells were operated at 90 °C. The cathode chamber was fed with oxygen at 239 kPa (20 psig) with a flow rate corresponding to five times that required by stoichiometry of the 4-electron oxygen reduction at the applied current density. Unless otherwise stated, the oxygen stream was humidified with 0.5 cm^3 min^{-1} of deionized water.

The anode compartment was not pressurized. The used brine and chlorine from the anode chamber were separated in a recirculation tank. The tank was equipped with an overflow and constantly fed with fresh purified brine (310 k m^{-3}, < 10 ppb Ca + Mg, Dow Chemical). Fresh and used brine were mixed thoroughly in the tank and part of the resulting solution was redirected to the cell while another part was collected for recycling. In this way, constant concentration of the feed solution was maintained. Unless otherwise stated, the feed concentration was 200 ± 3 kg m^{-3}. The estimated outlet brine concentration was approximately 186 kg m^{-3} at 10 kA m^{-2} and proportionally higher at lower current densities. The chlorine gas was scrubbed with a 18–20 weight % NaOH solution.

The peroxide content in the NaOH solution was determined spectrophotometrically. Fresh samples of sodium hydroxide were mixed with a known amount of potassium ferricyanide solution in aqueous NaOH. The peroxide content was determined from a decrease of ferricyanide absorption at 418 nm [29].

Caustic current efficiency was determined from titration of the sodium hydroxide samples with standardized 1.0 M HCl solution (Fisher) against phenolphthalein. Due to the very weak acidic properties of hydrogen peroxide ($pK_a = 11.75$ [30]), the volume of the acid used to neutralize the NaOH sample corresponded to the sum of the sodium hydroxide present in the sample and the NaOH produced as a result of hydroperoxide anion (HO_2^-) protonation. Since the latter quantity was also equal to the amount of NaOH that would form as a result of HO_2^- decomposition, the current efficiencies quoted in this paper are not corrected for peroxide.

Constant current electrolysis was performed using a Lambda LYS-K-5-0V power supply coupled to a Hewlett Packard 6060B electronic load-box. The load-box was also coupled to a high frequency resistance

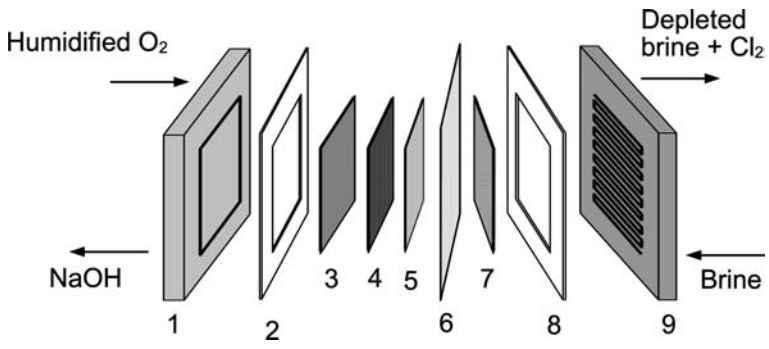

Fig. 1. Components of the electrochemical cell: 1 – cathode current collector, 2 – cathode gasket, 3 – cathode flow-field, 4 – gas diffusion cathode, 5 – carbon cloth spacer, 6 – cation exchange membrane, 7 – anode meshes, 8 – anode gasket, 9 – anode current collector and flow-field.

(HFR) measurement system that was comprised of a Voltech model TF200 frequency response analyzer and two Stanford Research Systems model SR560 low-noise preamplifiers for current and voltage signals. The system was controlled by Labview® software (National Instruments) installed on a MacIntosh computer. A cell voltage measurement was performed every 6 min and was immediately followed by a resistance measurement. In the latter case, a high frequency (2 kHz) ac signal of small amplitude (30 mV) modulated the voltage of the load-box and consequently the cell voltage and the current. The ratio of the ac components of the cell voltage and the current was assumed to be equal to the ion-exchange membrane resistance, hereafter called HFR. The error associated with this approximation was rather small, as the observed phase shift was typically in the range of 15–17°.

The system was also equipped with a Hewlett Packard model 3488A switch/control unit, a model 3421A data acquisition/control unit, as well as an IOTech model 488/4 serial bus converter. These were responsible for switching between the different modes of measurement, data acquisition from the two test stations, and data transfer to the computer.

3. Results

Figure 2 shows the cell voltage, HFR and cell voltage corrected for ohmic drop, obtained from a typical long-term test. After approximately 100 initial hours, where lower current densities were applied, the cell was operated at 10 kA m^{-2} without significant deterioration of its performance for around 660 h, when the experiment was terminated by an extended power outage. The current density of 10 kA m^{-2} is 2.5–3.3 times higher than the current densities used in industrial hydrogen-evolving membrane cells. Most of the data presented below were for this current density.

The observed decrease in high frequency resistance during the initial hours of electrolysis originates from the increase in current density and the associated increase in water transport through the membrane [31].

3.1. *Peroxide generation*

3.1.1. *Effect of catalyst loading and current density*

The cells were operated for approximately 24 h at five consecutive current densities of 2.0, 4.0, 6.0, 8.0, and 10 kA m^{-2} and the peroxide level was measured in the initial 3 h of operation at a given density. The peroxide content in the sodium hydroxide generated was found to increase with current density at both high (80% Pt, 0.05 kg m^{-2}) and low (20% Pt, 0.005 kg m^{-2}) catalyst loading (Figure 3). This effect is believed to originate from the different kinetics of complete 4-electron reduction and partial 2-electron reduction of oxygen:

$$O_2 + 2H_2O + 4e^- \rightarrow 4OH^- \quad (1)$$

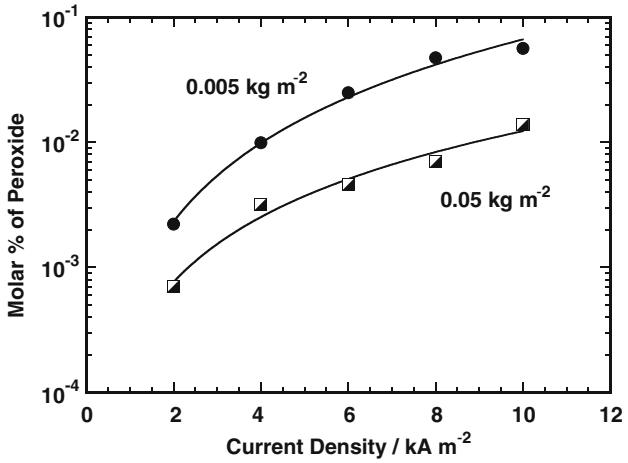

Fig. 3. Effect of current density and Pt loading on peroxide generation.

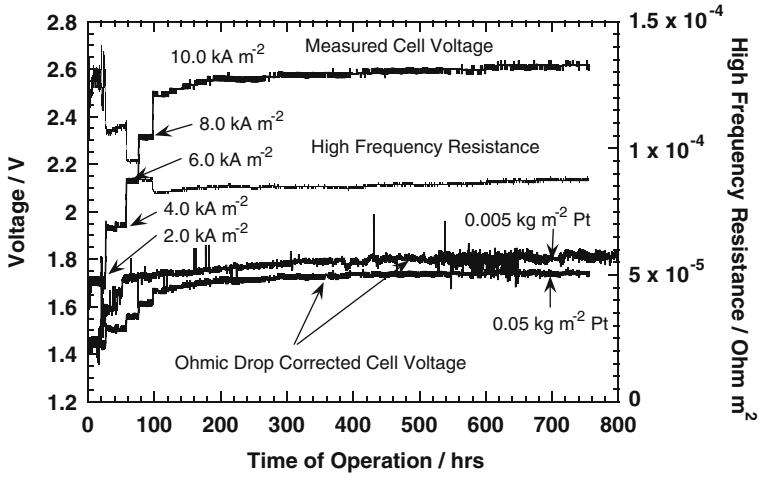

Fig. 2. Cell voltage, high frequency resistance and ohmic drop-corrected cell voltage in a typical long-term test of a 50 cm^2 cell. Platinum loading: 0.05 kg m^{-2}. Vertical sections of the plots correspond to different current densities. For comparison, ohmic drop corrected cell voltage for 0.005 kg m^{-2} Pt is also shown. See experimental section for other experimental conditions.

$$O_2 + H_2O + 2e^- \rightarrow OOH^- + OH^- \quad (2)$$

The increase of current density shifts the cathode potential towards the more negative values and affects the relative rates of peroxide and caustic generation.

The ratio of peroxide concentrations generated at high and low catalyst loadings is roughly independent of current density and its average value for the plots in Figure 3 equals 4.5. The ratio of peroxide concentrations generated at high and low catalyst loading qualitatively correlates with the relative contents of Pt in catalytic layers of both electrodes, and suggests that carbon and platinum particles compete as oxygen reduction centers. While the numbers of electrons involved in the ORR on individual Pt and C particles and their respective efficiencies of peroxide generation are unknown, the literature data clearly demonstrate that gas diffusion electrodes containing pure carbon in the catalyst layer produce significantly more peroxide than electrodes containing carbon supported Pt catalysts [11, 12, 24, 32, 33].

The slightly higher overpotentials of the oxygen cathodes with low Pt loadings may also contribute to the higher peroxide generation rates at low Pt loadings. The magnitude of this effect is rather small, since the observed differences in ohmic drop-corrected voltages amount to 0.05–0.08 V at 10 kA m^{-2} (Figure 2).

3.1.2. *Effect of electrolysis time*

The rate of peroxide generation depends on the electrolysis time. Peroxide concentration changes occur in times of tens to hundreds of hours and depend on experimental conditions. The typical dependence of peroxide concentration on electrolysis time is shown in Figure 4. We believe that the observed increase of peroxide generation at constant current density reflects the increasing role of carbon particles in oxygen reduction. The contribution from the carbon centers is likely to increase with time in the presence of peroxide [23], oxygen, and hot and concentrated caustic. These harsh conditions can lead to surface oxidation of the carbon particles and an increase of their hydrophilicity. Another likely reason for the higher contribution of carbon in peroxide generation at the cathode is the loss of platinum surface area due to agglomeration of Pt particles [33] and/or loss of Pt particles due to oxidative corrosion of carbon carriers [34].

A loss in hydrophobicity of the cathode was always observed after a life test, which ranges from a few hundred to 2000 h. The water contact angle on the catalyst side of the electrode before life test was approximately 147° and 170° on the gas diffusion layer side. The contact angle dropped below ~120° on the catalyst side and below ~140° on the gas diffusion layer side after electrolysis. These measurements were only rough estimates, because the contact angle varied considerably over the electrode surface due to inhomogeneity of the samples. In the areas, where the flow-field remained in direct contact with the sample, the gas diffusion layer exhibited exceptionally elevated hydrophilicity. When the electrode was rinsed, water frequently adhered to the electrode in the areas of contact and formed a pattern that was reproducing the geometry of the flow-field.

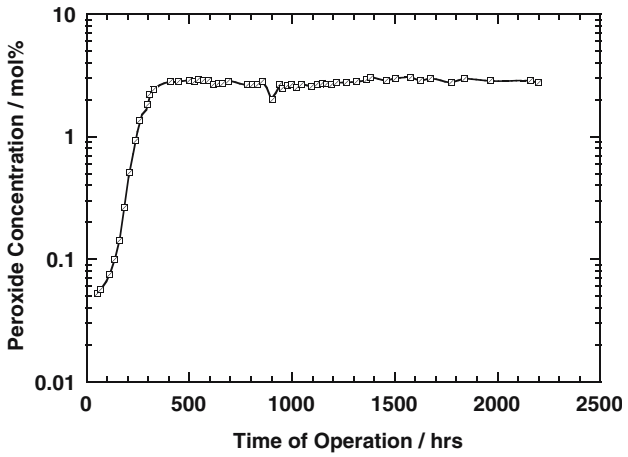

Fig. 4. Time effect on peroxide generation rate. Platinum loading: 0.005 kg m^{-2}. Current density: 10 kA m^{-2}.

The measurement of the contact angle on the catalyst side was distorted by another phenomenon. Prolonged electrolysis invariably resulted in some adhesion of the catalyst layer and the carbon cloth spacer. When the parts were being separated, numerous carbon fibers were transferred to the catalyst layer and some material from the catalyst layer was transferred to the carbon cloth. While the presence of the material from the catalyst layer on the hydrophilic spacer could be frequently seen with a naked eye, the presence of the carbon fibers on the electrode surface was detected using a microscope.

Even though the amount of material transferred from the catalyst layer to the spacer was rather small, no attempts were made to determine the quantity of platinum present in the catalyst layer after electrolysis, since such an experiment would not help understand the observed changes in peroxide generation rate at 10 kA m^{-2}. Our previous experiments, where the cells equipped with no spacer were used, frequently indicated some catalyst loss during electrolysis, in accordance with the data obtained by Morimoto et al. [34]. However, since the experiments at current densities above 2–4 kA m^{-2} required ''conditioning'' of the membrane at lower current densities to prevent its possible damage at higher current densities, any platinum loss determined after electrolysis always reflected the sum of losses in all current densities applied. Among them, the possible loss of platinum at 10 kA m^{-2} was most likely negligible [34] and masked by significantly larger losses resulting from the cell operation at lower current densities [34] during the initial hours of electrolysis.

An examination of the electrode after electrolysis under the microscope revealed also numerous cracks in

both the gas diffusion layer and the catalyst layer. The number of cracks per unit surface area seemed to be higher on the catalyst side of the electrode.

An attempt was undertaken to determine, if peroxide was predominantly responsible for the loss of electrode hydrophobicity. Small pieces of ELAT® were placed in three beakers containing: deionized water, 31% (weight) sodium hydroxide, and 31% (weight) sodium hydroxide with as high as possible quantity of peroxide added [35]. The temperature of the solutions was maintained at approximately 90 °C. Unfortunately, due to the fast peroxide decomposition, the experiment required frequent additions of peroxide and for this reason it could not be continued beyond 8 h. After such a short time, none of the samples exhibited any meaningful change in the contact angle.

3.1.3. *Effect of brine concentration*

The effect of brine concentration on peroxide production was studied at a current density of 10 kA m^{-2} for times longer than 500 h after a steady-state peroxide generation rate was reached (Figure 4). Brine concentration was adjusted by modifying the fresh brine supply to the recirculation tank. It usually took around an hour for the brine concentration to reach its steady-state level. For the purposes of hydroxide and peroxide analysis, samples of the caustic were taken after an additional one half to one hour after the brine concentration stabilized.

Figure 5 shows the effect of brine concentration on the composition of the NaOH solution generated. An increase of brine concentration from 136 to 228 kg m^{-3} produces an increase of NaOH concentration from around 26.5% to a little more than 31%. The peroxide content in the solution increases even faster, as manifested by approximately 25% increase of the peroxide-to-hydroxide molar ratio. As fully discussed in Section 4 below, the effect of brine on peroxide generation most likely results from changes in water activity at the oxygen reduction site caused by the NaOH concentration changes.

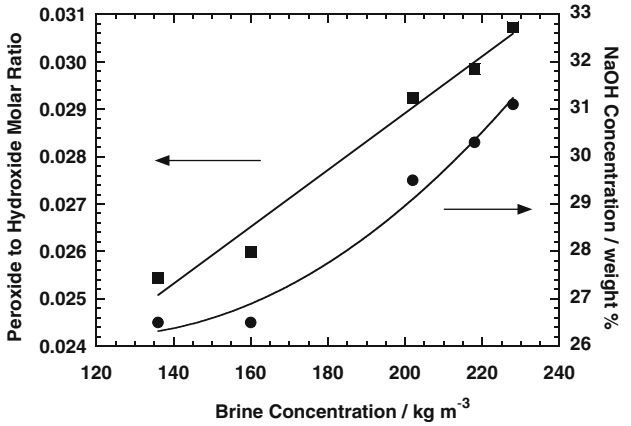

Fig. 5. Effect of brine concentration on peroxide generation rate and NaOH concentration. Platinum loading: 0.005 kg m^{-2}. Current density: 10 kA m^{-2}. Reproduced with permission from Abstracts of the 201st Meeting of the Electrochemical Society, Vol. 2002-1. Copyright 2002 The Electrochemical Society.

The effect of brine strength on NaOH concentration most likely results from changes in the membrane swelling. At lower brine concentrations, the membrane is more swelled and more permeable than at higher concentrations. As a consequence, more water is transported through the membrane [31] yielding lower caustic concentration. A more quantitative measure of the degree of membrane swelling and permeability is its resistance, which increases about 7% for the measured increase in brine concentration (Figure 6). As could be expected, the caustic current efficiency also increases with the brine concentration as a result of decreased caustic crossover (Figure 6).

One may also suspect the partial oxygen evolution [36, 37] on the DSA® anode to contribute to the above phenomena (Figures 5 and 6). This reaction produces hydronium cations and its relative contribution to the

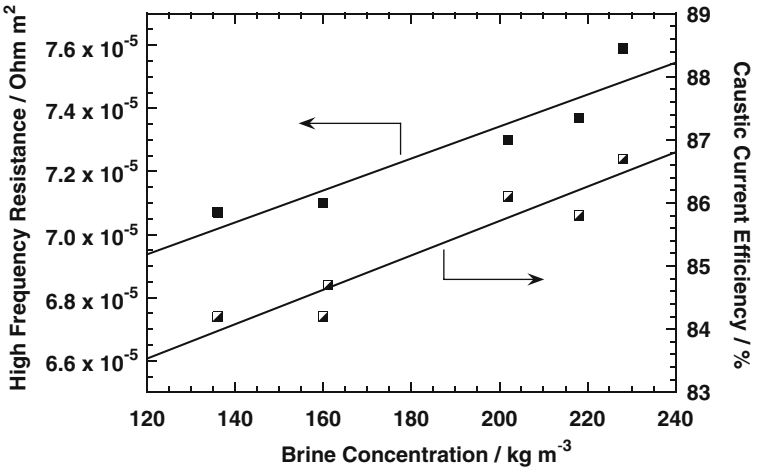

Fig. 6. Effect of brine concentration on membrane resistance and caustic current efficiency. Platinum loading: 0.005 kg m^{-2}. Current density: 10 kA m^{-2}.

measured current increases with the decrease in brine concentration [36, 37]. The increase in the brine acidity may produce an increased H_3O^+ flux across the membrane, which may result in a lower membrane resistance, lower current efficiency, and lower NaOH concentration. Such an explanation would be plausible for a sulfonated membrane, which behaves like a strong electrolyte in both the acid and the sodium salt form and its conductivity correlates with the molar conductivities of hydronium and sodium ions [38]. The picture seems more complex in the present case. As the carboxylic layer of the bi-layer membrane behaves like a weak electrolyte when in the protonated form, the net effect of the enhanced oxygen evolution and the increased brine acidity may be opposite to the effect observed. Consequently, the effect of brine concentration on the extent of the membrane swelling offers a better explanation of the effects shown in Figures 5 and 6.

One should note that the current efficiencies in Figure 6 are generally lower than the current industrial standard for membrane cells, i.e., 93–95%. The lower current efficiencies in present experiments result predominantly from the much higher current densities applied in our cells (10 kA m^{-2}) than those typically used in industrial membrane cells (3.0-4.0 kA m^{-2}). The current efficiencies measured by us for 200 kg m^{-3} feed brine at lower current densities were: ~95%, 93%, 92%, and 91% for 2.0, 4.0, 6.0, and 8.0 kA m^{-2}, respectively. Higher current densities are likely to decrease caustic current efficiency by increasing membrane swelling and permeability [31], by more significant contribution of the oxygen evolution reaction as well as by membrane blinding by chlorine gas. Some modifications of our cells have recently resulted in a significant improvement of caustic current efficiency.

3.1.4. *Effect of oxygen stream humidification*

The significant change in oxygen humidification level from 0 to almost 6 cm^3 min^{-1} decreases the peroxide-to-hydroxide molar ratio by approximately 10%. At the same time, caustic concentration drops from 31.6% to 12.6%, i.e., much more than observed in experiments where the brine concentration effects were studied (see above). Quantitative comparison of the humidification and brine concentration effects on peroxide formation is shown in Figure 7. Here, the molar ratio of peroxide-to-hydroxide is plotted against NaOH concentration, which is a common measure of the quantity of water introduced into the cathode compartment either by transport from the anode compartment through the membrane or by direct humidification of the oxygen stream. The much weaker effect of the direct humidification of oxygen (Figure 7) indicates that most of the humidification water does not reach the catalyst layer and thus affects neither the composition of the liquid phase at the reaction site nor the membrane permeability (see also Section 3.2.2 below). The main effect of oxygen humidification is the diluting of the NaOH solution that already left the electrode.

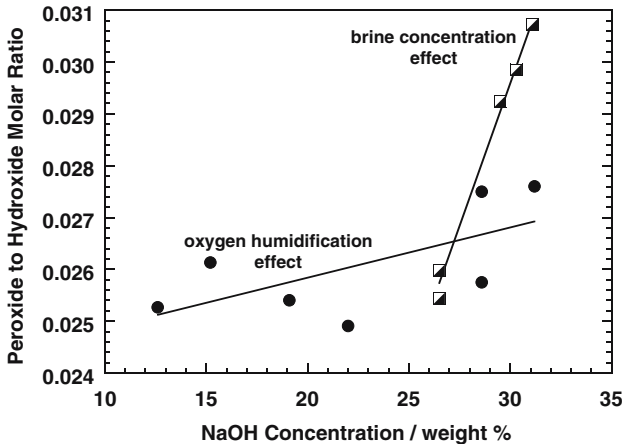

Fig. 7. Comparison of effects of oxygen stream humidification and brine concentration on peroxide generation rate. Platinum loading: 0.005 kg m^{-2}. Current density: 10 kA m^{-2}.

3.1.5. *Effects of the hydrophilic spacer and the oxygen flow rate*

The hydrophilic spacer significantly reduces peroxide generation (Figure 8). We believe that the presence of spacer reduces likelihood of carbon particles participating in the oxygen reduction in two ways. First of all, since the spacer acts as an efficient drain for NaOH solution [39], the quantity of NaOH remaining inside the electrode decreases and corrosion of carbon particles is less likely to occur. Secondly, without the spacer, the catholyte can accumulate in the pores of the catalyst-free gas diffusion layer, and partial reduction of oxygen may occur on carbon particles inside the gas diffusion layer.

The above conclusion seems to be supported by another observation. We found that the decrease of oxygen flow in the cathode compartment from five to two times of that required by the stoichiometry of reaction 1 reversibly increases the peroxide generation at

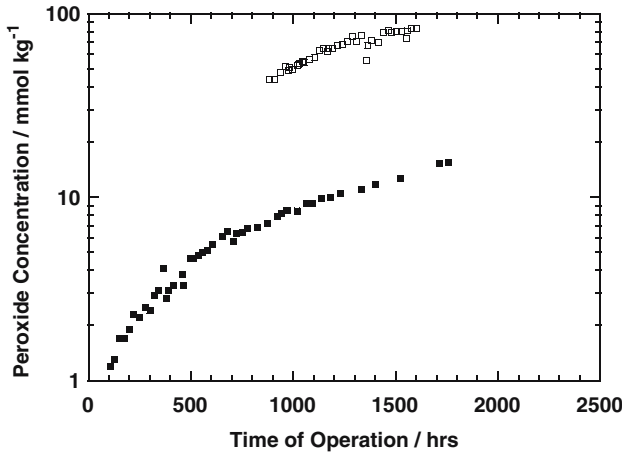

Fig. 8. Effect of the hydrophilic spacer on peroxide generation rate. Platinum loading: 0.05 kg m^{-2}. Current density: 10 kA m^{-2}. Cell with no spacer – open symbols. Cell with hydrophilic spacer – full symbols.

10 kA m^{-2} by a factor of two. Unlike the pressure in the cathode chamber, the flow rate cannot have a direct effect on the reaction stoichiometry. Consequently, we postulate that high velocity of oxygen in the cathode chamber helps removing NaOH solution from the pores of the gas diffusion layer and it thus has a similar effect on peroxide generation as the spacer.

3.2. *Chloride transport through the membrane*

Sodium chloride is a major impurity of the sodium hydroxide produced in diaphragm chlor-alkali cells, but it is also present in much smaller quantities in the NaOH obtained from the membrane process. The presence of chloride in the solution may have adverse effects on the operation of the oxygen-depolarized chlor-alkali cell, because chloride is a known inhibitor of the 4-electron reduction of oxygen. In similarity to other inhibitors of oxygen reduction, chloride promotes partial, 2-electron reduction of oxygen to peroxide [40, 41]. The effects of the cell operating conditions on chloride content in the NaOH and its potential effects on peroxide generation are described below.

3.2.1. *Current density effect*

The concentration of chloride in a NaOH solution decreases substantially with the increase in current density (Figure 9). Since chloride anions are transported to the cathode compartment by diffusion and electroosmotic flow, and negated by migration [42], the observed effect indicates the predominant role of migration in the observed changes of chloride content in the caustic product. This effect cannot be correlated with peroxide formation, as different current densities correspond to different kinetics of oxygen reduction.

3.2.2. *Oxygen humidification effect*

Within the limits of experimental error, there was no effect of oxygen humidification on the chloride content in the NaOH solution other than dilution, i.e., the ratio of Cl^- to the NaOH concentration remained virtually insensitive to the humidification level. In similarity to the humidification effect on the peroxide generation rate (see above), this result reflects the ineffectiveness of the humidification, i.e., its rather weak effect on the composition of the liquid phase at the membrane/catalyst layer interface.

3.2.3. *Brine concentration effect*

As opposed to a predicted decrease of the NaCl content in the NaOH with brine concentration [42], the chloride concentration was found to be rather insensitive to brine concentration changes within the range of 160–205 kg m^{-3}. The NaCl concentrations were scattered between 18.5 and 24.4 ppm. Similarly, no definite trend could be detected for the NaCl contents normalized for NaOH concentration – the latter varied between 26.5% and 30.1% for the above brine concentration range.

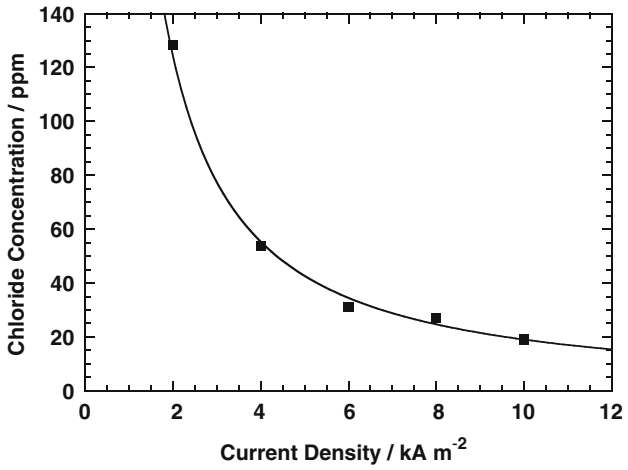

Fig. 9. Effect of current density on chloride concentration in caustic soda. Chloride content is measured for samples taken during the first 24 h of cell operation at the given current density. Platinum loading: 0.005 kg m^{-2}.

Because brine concentration was shown to be a major factor determining membrane swelling and permeability (Section 3.1.3), the lack of detectable effects of brine concentration on the NaCl content in the sodium hydroxide solution seems surprising. It may suggest that the opposite effects of chloride concentration (driving force) and ionic strength (membrane swelling and permeability) on chloride transport through the membrane cancel at high current densities. Also, the chloride concentration in the NaOH may be elevated due to the transfer of chlorate, hypochlorite, or both from the anode compartment and their subsequent chemical or electrochemical reduction to chloride in the cathode compartment. The magnitude of this effect is most likely small [42].

3.2.4. *Time effect*

The concentration of chloride in a NaOH solution generated at 10 kA m^{-2} seems to decrease after 1500 h (Figure 10) of electrolysis, but the magnitude of this decrease is unclear. As the opposite effect may be expected for a prolonged cell operation at high current densities [31], the decrease in chloride concentration may be associated with changes in current distribution over the membrane surface [42]. Some regions of the membrane may be initially inactive due to incomplete wetting of the carbon cloth/electrode interface. Such regions exhibit increased carry over of anions because of lowered local current densities [42]. A gradual increase in the hydrophilicity of the electrode may decrease the surface area of the inactive regions and lead to a more even current distribution and a decrease of chloride crossover. The small decrease of chloride concentration (Figure 10) in the NaOH seems to have no effect on the peroxide generation rate (Figure 4).

The lack of correlation between the peroxide generation rate and chloride crossover is clearly visible at the shorter electrolysis times. Figure 11 presents time

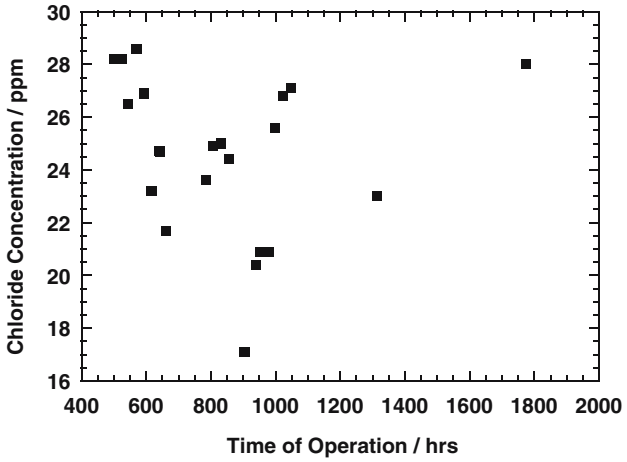

Fig. 10. Time effect on chloride concentration in caustic soda during a long-term test. Platinum loading: 0.005 kg m^{-2}. Current density: 10 kA m^{-2}.

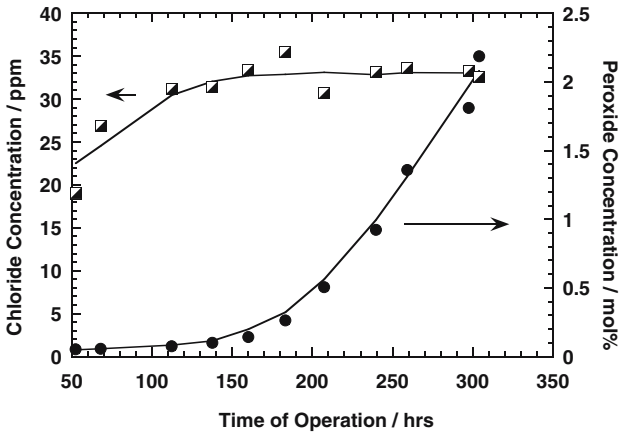

Fig. 11. Changes of chloride and peroxide concentrations in caustic soda during the first 300 h of cell operation at 10 kA m^{-2}.

dependencies for the concentrations of chloride and peroxide in the NaOH solution generated at 10 kA m^{-2} during the first 300 h of cell operation. During this time the most significant changes in peroxide concentration occur (Figure 4). At the same time, the chloride content does not vary, except for the first 20 h at 10 kA m^{-2} (between 50 and 70 h after the start of electrolysis), where the membrane may not have attained its steady state permeability. These results demonstrate the insignificance of the chloride effect on peroxide generation.

4. General discussion and conclusions

As shown in the preceding sections, the important factors that determine formation of peroxide in our chlor-alkali cells are: (i) catalyst loading, (ii) current density, (iii) time, (iv) composition of the solution at the reaction site, and (v) quantity and distribution of the solution inside the gas diffusion cathode. The observed effects of catalyst loading and current density on peroxide generation seem to have a rather obvious explanation based on the relative kinetics of the 4-electron and 2-electron reduction of oxygen on the surfaces of different catalysts (platinum vs. carbon) and at different overpotentials, respectively. The effects of time and catholyte composition on peroxide generation require additional discussion.

The interpretation of the time effect based on the increase of carbon active area vs. that of platinum seems most reasonable. Of the two materials, platinum and carbon, the latter is much more susceptible to chemical attack in a strongly oxidizing and hot environment. Due to their increased hydrophilicity, the surface oxidized carbon particles can become oxygen reduction centers. However, any chemical process – including oxidation – that can modify hydrophilicity of the carbon surface, is also likely to modify the ability of carbon to support platinum. In the worst case, the modified carbon surface may no longer support Pt particles and an irreversible loss of platinum may occur. The magnitude of such a phenomenon was shown [34] to decrease with an increase in cathode overpotential (current density), and with a decrease in the degree of graphitization of the carbon support. While the data in Ref. [34] suggest that the catalyst loss due to the oxidative corrosion of carbon carriers and platinum dissolution should be negligible at high current densities, some effect of these phenomena on the observed time dependence of the peroxide generation rate cannot be excluded.

Another effect, which may have led to some decrease of platinum surface area vs. that of carbon, is platinum particle agglomeration, which was shown [33] to occur at elevated temperatures in strongly alkaline media. However, this process seems to occur during only the first 24 h of electrolysis [33].

On the other hand, the results in Section 3.1.5 demonstrate that quantity and distribution of NaOH inside the electrode have a very significant effect on the peroxide generation rate. The inefficient transport of NaOH from the cathode in cells without the spacer and/or at low oxygen velocities leads to an increase of the carbon surface area in contact with NaOH solution and to a significant increase in the peroxide generation. Since the increase in hydrophilicity of carbon particles increases the surface area of carbon in contact with NaOH, it is expected to lead to an increase of the peroxide generation rate as well. A contribution to the variation of the catalytic/surface properties of carbon particles from possible chloride poisoning [43] cannot be excluded either. Most likely, carbon particles in both the catalyst layer and the gas diffusion layer contributed to the observed phenomena.

There seems to be no correlation between the chloride and peroxide levels in the caustic (Section 3) unless chloride adsorption is significantly slower than the observed chloride concentration changes in the caustic stream (Figure 11). Such an effect is highly unlikely in the case of platinum. Hence, the observed time effect on peroxide generation cannot be attributed to the

inhibition of 4-electron oxygen reduction (Equation 1) by the progressive accumulation of chloride on the platinum surface. Consequently, the observed changes in the peroxide generation rate shown in Figure 11 originate from the increasing contribution of the oxygen reduction process on carbon particles.

Another potential source of the time dependence of peroxide generation might be the poisoning of the Pt surface by chlorates that gradually accumulate in the recirculation tank [44] as a result of slow homogeneous reactions [45]. Unfortunately, the chlorate concentration in the recirculation tank was not monitored. Based on the comparison of chloride and perchlorate adsorption on platinum [46], one may expect that chlorate is more weakly adsorbed than chloride. Hence, the effects resulting from chlorate adsorption should be generally weaker than those expected for chloride and therefore can hardly be responsible for the time effect on peroxide generation. Based on similar argumentation, the observed brine concentration effect on peroxide generation most likely does not originate from changes in chlorate adsorption.

We believe that the brine concentration effect on peroxide generation results from the associated changes in NaOH concentration (Figure 5) at the reaction site. In fact, concentrated sodium hydroxide is a medium of a low and strongly concentration-dependent water activity [47]. While the complete 4-electron reduction of oxygen to hydroxide requires 2 mol of water per 1 mol of oxygen (Equation 1), its partial reduction (Equation 2) requires two times less water. An increase in the caustic concentration is accompanied by a decrease in water activity, which makes the reaction 2 more favorable. This interpretation seems supported by a recent paper by Chatenet et al. [33]. Their study of oxygen reduction on Pt in NaOH solutions revealed more significant peroxide formation in 11.1 M than in 1.0 M solution.

Acknowledgements

Financial support from the Department of Energy's Industrial Technologies Program (formerly Office of Industrial Technologies) is greatly appreciated. Thanks are also due to Rich Varjian and Harry Burney of Dow Chemical for frequent discussions, brine and membrane supply and chloride analysis, as well as to Amanda Casteel and Sarah Stellingwerf for their help in some experiments. Part of this research was presented during the centennial meeting of the Electrochemical Society [48].

References

1. K. Yamaguchi, Chlor-alkali technologies applied in Japan, *in* H.S. Burney, N. Furuya, F. Hine and K.-I. Ota (Eds), Chlor-Alkali and Chlorate Technology: R.B. MacMullin Memorial Symposium, 196th Meeting of the Electrochemical Society, Hawaii, October (1999), Electrochemical Society Proceedings, Vol. 99-21, pp. 127–144.
2. L.Q. Mao, K. Arihara, T. Sotomura and T. Ohsaka, *Electrochim. Acta* **49** (2004) 2515.
3. Y. Yang and Y. Zhou, *J. Electroanal. Chem.* **97** (1995) 271.
4. S. Štrbac and R.R. Adžić, *J. Electroanal. Chem.* **403** (1996) 169.
5. Y.-F. Yang, Y.-H. Zhou and C.-S. Cha, *Electrochim. Acta* **40** (1995) 2579.
6. S. Štrbac and R.R. Adžić, *Electrochim. Acta* **41** (1996) 2903.
7. C.-C. Chang, T.-C. Wen and H.-J. Tien, *Electrochim. Acta* **42** (1997) 557.
8. K. Tammeveski, T. Tenno, J. Claret and C. Ferrater, *Electrochim. Acta* **42** (1997) 893.
9. L. Geniès, R. Faure and R. Durand, *Electrochim. Acta* **44** (1998) 1317.
10. J. Perez, E.R. Gonzalez and E.A. Ticianelli, *Electrochim. Acta* **44** (1998) 1329.
11. I. Morcos and E. Yeager, *Electrochim. Acta* **15** (1970) 953.
12. Z.W. Zhang, D. Tryk and E. Yeager, *J. Electrochem. Soc.* **130** (1983) C333.
13. J. Ponce, J.-L. Rehspringer, G. Poillerat and J.L. Gautier, *Electrochim. Acta* **46** (2001) 3373.
14. L. Nei, *Fresenius J. Anal. Chem.* **367** (2000) 436.
15. J.J. Podestá and C.V. Piatti, *Int. J. Hydrogen Energ.* **22** (1997) 753.
16. J.-D. Kim, S.-I. Pyun, T.-H. Yang and J.B. Ju, *J. Electroanal. Chem.* **383** (1995) 161.
17. J. Xu, W. Huang and R.L. McCreery, *J. Electroanal. Chem.* **410** (1996) 235.
18. H.-K. Lee, J.-P. Shim, M.-J. Shim, S.-W. Kim and J.-S. Lee, *Mater. Chem. Phys.* **45** (1996) 238.
19. C.-C. Chang and T.-C. Wen, *Mater. Chem. Phys.* **47** (1997) 203.
20. R. Beckmann and B. Lüke, Know-how and Technology – Improving the Return on Investment for Conversions, Expansions and New Chlorine Plants, *in* J. Moorhouse (Ed.), Modern Chlor-Alkali Technology, Proceedings of the 2000 London International Chlorine Symposium Organized by SCI's Electrochemical Technology Group, London, UK, 31st May–2nd June (2000), Vol. 8, (Blackwell Science, 2001), pp. 196–212.
21. N. Furuya and H. Aikawa, *Electrochim. Acta* **45** (2000) 4251.
22. F. Federico, G.N.Martelli and D.Pinter, Gas-diffusion Electrodes for Chlorine-related (Production) Technologies, *in* J. Moorhouse (Ed.), Modern Chlor-Alkali Technology, Proceedings of the 2000 London International Chlorine Symposium Organized by SCI's Electrochemical Technology Group, London, UK, 31st May–2nd June (2000) (Blackwell Science, 2001), pp. 114–127.
23. M. Sugiyama, K. Saiki, A. Sakata, H. Aikawa and N. Furuya, *J. Appl. Electrochem.* **33** (2003) 929.
24. O. Ichinose, M. Kawaguchi and N. Furuya, *J. Appl. Electrochem.* **34** (2004) 55.
25. X. Ren, P. Zelenay, S. Thomas, J. Davey and S. Gottesfeld, *J. Power Sources* **86** (2000) 111.
26. A. Sakata, M. Kato, K. Hayashi, H. Aikawa and K. Saiki, Long Term Performances of Gas Diffusion Electrode in Laboratory Cells, *in* H.S. Burney, N. Furuya, F. Hine and K.-I. Ota (Eds), Proceedings of the Chlor-Alkali and Chlorate Technology: R.B. MacMullin Memorial Symposium, 196th Meeting of the Electrochemical Society, Hawaii, October (1999), Electrochemical Society Proceedings, Vol. 99-21, pp. 223–233.
27. O. Ichinose, H. Aikawa, T. Watanabe and A. Uchimura, Pilot Cell Scale Manufacture of the Gas Diffusion Electrode, *in* H.S. Burney, N. Furuya, F. Hine and K.-I. Ota (Eds), Proceedings of the Chlor-Alkali and Chlorate Technology: R.B. MacMullin Memorial Symposium, 196th Meeting of the Electrochemical Society, Hawaii, October (1999), Electrochemical Society Proceedings, Vol. 99-21, pp. 216–222.
28. K. Saiki, A. Sakata, H. Aikawa and N. Furuya, Reduction in Power Consumption of Chlor-Alkali Membrane Cell Using Oxygen Depolarized Cathode, *in* H.S. Burney, N. Furuya, F. Hine and K.-I. Ota (Eds), Proceedings of the Chlor-Alkali and Chlorate

Technology: R.B. MacMullin Memorial Symposium, 196th Meeting of the Electrochemical Society, Hawaii, October (1999), Electrochemical Society Proceedings, Vol. 99-21, pp. 188–195.
29. F. Aziz and G.A. Mirza, *Talanta* **11** (1964) 889.
30. M. Ardon, *in* R.A. Plane and M.J. Sienko (Eds), 'Oxygen. Elementary Forms and Hydrogen Peroxide, The Physical Inorganic Chemistry Series' (W.A. Benjamin, New York, Amsterdam, 1965).
31. J.T. Keating and H.M.B. Gerner, High Current Density Operation – The Behavior of Ion Exchange Membranes in Chloralkali Electrolyzers, *in* S. Sealey (Ed.), Modern Chlor-Alkali Technology, Proceedings of the 1997 London International Chlorine Symposium Organized by SCI Electrochemical Technology Group, London, UK, 4th–6th June (1997), Vol. 7, (SCI 1998), pp. 135–144.
32. P.S.D. Brito and C.A.C. Sequeira, *J. Power Sources* **52** (1994) 1 and references therein.
33. M. Chatenet, L. Genies-Bultel, M. Aurousseau, R. Durand and F. Andolfatto, *J. Appl. Electrochem.* **32** (2002) 1131.
34. T. Morimoto, K. Suzuki, T. Matsubara and N. Yoshida, *Electrochim. Acta* **45** (2000) 4257.
35. Solid peroxide had to be frequently added to the reaction vessel, because it decomposed rapidly on the ELAT® surface at 90 °C. The estimated peroxide content in the solution was around 0.1 M.
36. L.R. Czarnetzki and L.J.J. Janssen, *J. Appl. Electrochem.* **22** (1992) 315.
37. J.L. Fernández, M.R. Gennero de Chialvo and A.C. Chialvo, *J. Appl. Electrochem.* **32** (2002) 513.
38. P. Vanýsek, *in* 'CRC Handbook of Chemistry and Physics', 81st edn. (CRC Press, 2000).
39. T. Shimamune, K. Aoki, M. Tanaka, K. Hamaguchi and Y. Nishiki, U.S. Patent 6117286.
40. T.J. Schmidt, U.A. Paulus, H.A. Gasteiger and R.J. Behm, *J. Electroanal. Chem.* **508** (2001) 41 and references therein.
41. V. Stamenkovic, N.M. Markovic and P.N. Ross Jr., *J. Electroanal. Chem.* **500** (2001) 44.
42. C.-P. Chen and B.V. Tilak, *J. Appl. Electrochem.* **26** (1996) 235.
43. C. Ponce de Leon and D. Pletcher, *Electrochim. Acta* **41** (1996) 533.
44. S.A. Perusich and S.M. Reddy, *J. Appl. Electrochem.* **31** (2001) 421.
45. S.V. Evdokimov, *Russ. J. Electrochem.* **37** (2001) 786.
46. M.C. Santos, D.W. Miwa and S.A.S. Machado, *Electrochem. Comm.* **2** (2000) 692.
47. K. Kimoto, *J. Electrochem. Soc.* **130** (1983) 334.
48. L. Lipp, S. Gottesfeld and J. Chlistunoff, Abstracts of the 201st Meeting of the Electrochemical Society, Vol. 2002-1, Abstract 1117.